Food and Chemical Toxicology 132 (2019) 110644

Contents lists available at ScienceDirect

Food and Chemical Toxicology

journal homepage: www.elsevier.com/locate/foodchemtox

CDK2 and Bcl-xL inhibitory mechanisms by docking simulations and anti-tumor activity from piperine enriched supercritical extract

Valdelúcia M.A.S. Grinevicius[a], Kátia S. Andrade[b], Nádia S.R.S. Mota[a], Lizandra C. Bretanha[c], Karina B. Felipe[d], Sandra R.S. Ferreira[b], Rozangela C. Pedrosa[a,*]

[a] Laboratório de Bioquímica Experimental, Departamento de Bioquímica, Universidade Federal de Santa Catarina, Florianópolis, SC, Brazil
[b] Laboratório de Termodinâmica e Extração Supercrítica, Departamento de Engenharia Química e Engenharia de Alimentos, Universidade Federal de Santa Catarina, Florianópolis, SC, Brazil
[c] Laboratório de Eletroforese Capilar, Departamento de Química, Universidade Federal de Santa Catarina, Florianópolis, SC, Brazil
[d] Laboratório de Fisiologia e Sinalização Celular, Universidade Federal Do Paraná, Curitiba, PR, Brazil

ARTICLE INFO

Keywords:
Piper nigrum
Supercritical carbon dioxide extraction
Piperine
Molecular docking
CDK2/Bcl-xL
Anti-Tumor activity

ABSTRACT

Supercritical fluid technologies offer an innovative method for food industry and drug discovery from natural sources. The aim of the study is to investigate the anti-tumor activity of piperine rich extract by supercritical fluid (SFE) from black pepper (*Piper nigrum*). *In silico* docking simulations predicted anti-tumor molecular mechanism and protein-piperine hydrophobic interactions, showing hydrogen bonds between piperine and residue Ser5 inside the ATP binding site in CDK2. Moreover, piperine interacts with peptide substrate residue Lys8 inside its binding site in Cyclin A molecule. Other predicted interaction showed piperine inside the hydrophobic groove of Bcl-xL. Confirming the docking simulation, *in vitro* assays with SFE (40 °C/30 MPa) showed cytotoxicity to MCF-7 cells (IC50 = 27.8 ± 6.8 μg/ml) correlated to increased apoptosis. Balb/c mice-bearing Ehrlich Ascites Carcinoma (EAC) group that received the SFE (100 mg/kg/day) showed tumor growth inhibition (60%) and increased mice survival (50%), probably related to cell cycle arrest (G2/M) and increased apoptosis. *In vivo* treatments with SFE increased the expression of pro-apoptotic proteins (p53 and Bax), inhibited cell cycle proteins (CDK2, Cyclin A) and anti-apoptotic protein (Bcl-xL). Thus, confirming *in silico* predicted inhibitory interactions. These results clearly showed promising performance of the piperine-rich fraction recovered from black pepper, drawing attention to its use as complementary therapy for cancer.

1. Introduction

The natural products have been used as a source of food and traditional medicines for thousands of years. *Piper nigrum* L. (Piperaceae) or black pepper is a climbing shrub from India widely cultivated in the world as a spice commodity. Human survival and spice phytocompounds had millennial interconnections derived from its traditional use to combat foodborne-microorganisms and to reduce food poisoning (Sherman and Billing, 1999). Indeed, patterns of use and consumption of spice showed high proportions of black pepper (*P. nigrum* fruits) as a flavoring and antimicrobial ingredient of meat-based recipes (Sherman and Billing, 1999). Besides, black pepper had medicinal properties (Chaveerach et al., 2006) and their berries are key elements inside herbal formulae for treatment of disturbs in gastrointestinal tract and inflammation (Kurian, 2012) as well can be applied to breast cancer palliative care and adjuvant therapy (Liao et al., 2013).

Nowadays cancer patients are stimulated to adopt some alternative and complementary therapy based on the use of prebiotics, vitamins, minerals and phytochemical products extracted from herbs (Clarke et al., 2015). Prebiotic activity of piperine in black pepper extract can enhance the gastrointestinal health (Lu et al., 2017).

Piperine is the major alkamide present in Piper species with *in vitro* cytotoxicity against breast cancer cells and inhibiting *in vivo* breast cancer growth (Lai et al., 2012). Green extraction methods represent a group of extraction techniques for products and by-products valorization based on green and sustainable technologies, which innovation and improvements are based on process optimization and the use of alternative solvents like supercritical carbon dioxide (Chemat et al., 2012). Carbon dioxide (CO_2) is safe, readily available and the most used supercritical fluid, for a technology free of polluting organic solvents and, consequently, with reduced post-processing costs (Attard et al., 2015). Supercritical carbon dioxide enabled a fast and efficient piperine

* Corresponding author.
E-mail address: rozangela.pedrosa@ufsc.br (R.C. Pedrosa).

https://doi.org/10.1016/j.fct.2019.110644
Received 9 May 2019; Received in revised form 21 June 2019; Accepted 23 June 2019
Available online 26 June 2019

recovery from black pepper (Andrade et al., 2017). Moreover, SFE is a viable alternative to obtain high quality substances present in plant-derived by-products in food industries (Mota et al., 2018).

To address the anti-tumor potential of molecular interactions between ligands and macromolecules it is possible to use computational simulation, which reproduces chemical potential and determine the bound conformation and predict the binding energy (Trott and Olson, 2010). Due to its relevance, docking can support the discovery, design and development of new drugs and nutraceuticals starting with bioactive fractions from plants extracts. Thus, docking enables to detect probable binding sites for piperine inside ligand-protein complex. Target proteins were cell cycle progression protein Cyclin Dependent Kinase 2 (CDK2) and anti-apoptotic protein Bcl-xL. A search for inhibitors capable to act against these two proteins can be a viable approach to control cancer cells growth. CDK2-Cyclin A heterodimers play a critical role in signaling progression, providing phosphorylation signals to push cell cycle through S phase (Jacobsen et al., 2012). Besides, catalytic cycle of activated CDK2-cyclin A depends on the binding of protein substrate, ATP and Mg^{2+} ions acting as stabilizer of ATP binding (Jacobsen et al., 2012). While Bcl-xL pro-survival signals depend on the formation of Bcl-xL heterodimer with Bax which inhibits the formation of Bax oligomer to prevent apoptosis (Bertini et al., 2011).

Therefore, this study aims to use docking simulations to predict molecular mechanisms related to anti-tumor activity of piperine rich fraction obtained by supercritical carbon dioxide ($scCO_2$) from *Piper nigrum*. In order to confirm the computational response, *in vitro* and *in vivo* assays were conducted to evaluate the cytotoxic, anti-proliferative and anti-tumor effects of black pepper extract rich in piperine.

2. Materials and methods

2.1. Chemicals

Antibiotics, Dulbecco's modified Eagle medium (DMEM), Dubecco's Phosphate Buffered Saline (PBS) and fetal bovine serum (FBS) were purchased from GIBCO, Life Technologies (USA) (Cultilab, Campinas, SP; Brazil). Bromophenol blue, bovine serum albumin (BSA), dimethyl sulfoxide (DMSO), ethidium bromide (EtBr), propidium iodine (PI), the protease inhibitor cocktail, tetrazolium salt (MTT) are purchased from Sigma–Aldrich Brazil Ltda (São Paulo – SP, Brazil). Calbiochem (Merck, Rio de Janeiro – RJ, Brazil) provided phosphatase inhibitor cocktail. Rabbit polyclonal antibodies specific for anti-actin (Cat. sc-7210), for anti-cyclin A (Cat.sc-596) and anti-p53 (Cat. sc-6243) and mouse polyclonal antibodies specific for anti-Bax (Cat. sc-7480) and anti-Bcl-xL (Cat. Sc-8392) come from Santa Cruz Biotechnology, Inc. (Campinas - SP, Brazil). Goat polyclonal secondary antibodies for anti-rabbit IgG (Cat. AP132P) and for anti-mouse IgG (Cat. AP181P) as well as the chemiluminescence detection kit of HRP-coupled antibodies were purchased from Merck Millipore (Cotia, SP - Brazil). Other chemicals were American Chemical Society grade reagents.

2.2. Black pepper SFE and phytochemistry

The $scCO_2$ was performed using a high-pressure unit and procedure as presented in literature (Andrade et al., 2017). Shortly, the scCO2 extraction consisted of placing a fixed mass of 20 g of the dried grinded black pepper inside the extractor cell to form the fixed bed of particles, followed by the control of the process variables (temperature and pressure). The SFE with CO2 was conducted at temperature of 40 °C and pressure of 30 MPa, at constant solvent flow rate of 8 ± 2 g min − 1. The extraction time was set at 4 h according to the kinetic extraction curve. SFE phytochemical composition was determined by HPLC and CG/MS, with piperine and other compounds (30–750 Da) identified and presented in previous studies (Andrade et al., 2017; Grinevicius et al., 2017).

2.3. Molecular docking studies

Computational docking is widely used for study of protein-ligand interactions and for drug discovery and development (Forli et al., 2016). Protein preparations were done with AutoDock MGL Tools version 1.5.6. Statistical scoring function based in local search method of AutoDock Vina version 1.1.2 were applied to all docking score calculations (Trott and Olson, 2010; Forli et al., 2016). Docking parameters were kept at their default values. Thus, a sequence of preliminary grid-based exploratory evaluation provided values of binding energy of conformations. Then, ligand poses with lowest binding affinity energy were selected. Finally, its coordinates in the protein chain were the center of grid box or search space for docking (Forlemu et al., 2017). Final search box was large enough for the ligand to rotate in (Morris et al., 2009). Besides, to avoid bias, 5 Å were added randomly in all considered dimensions of grid box (Trott and Olson, 2010). Two proteins were the target for *in silico* analysis. The first was the phosphorylated complex CDK2-cyclin A-Peptide substrate (PDB 1QMZ) (resolution 2.2 Å; pH 7.0) (Brown et al., 1999). Second target protein was Bcl-xL (PDB 4TUH) (resolution 1.8 Å; pH 6.5) (Koehler et al., 2014).

Piperine is the major secondary metabolite found in supercritical carbon dioxide extract from black pepper (*Piper nigrum* L. cultivar Bragantina) (Grinevicius et al., 2017). For these reasons, piperine was the ligand used during *in silico* studies. The ligand piperine structure provided by PubChem Data Base (PuchChem CID 638024) was minimized using Open Babel version 2.4.1 with force field GAFF (O'Boyle et al., 2011). Molecular interactions were visualized with PyMOL version 1.8. x Open Source (The PyMOL Molecular Graphics System, Schrödinger, LLC). Predicted binding modes of flexible ligand with lowest-energy binding affinity were visualized with LigPlot + 0.8 software (Laskowski and Swindells, 2011) and with PyMOL version 1.8. x Open Source. Then, protein-ligand analysis also used scoring one function of AutoDock Vina. It predicted intermolecular contributions related to hydrophobic interactions and hydrogen bonds (Trott and Olson, 2010).

2.4. Black pepper SFE effects on viability, proliferation and cell death type

Human breast carcinoma (MCF-7) cell line (Rio de Janeiro cell bank, Brazil) were seeded (10^4 cells/well; 96 wells/plate) and kept in DMEM supplemented with fetal bovine serum (10%) and antibiotics penicillin (100 U/ml) and streptomycin (100 µg/ml) to allow confluence at standard conditions (24 h; 37 °C) under controlled atmosphere containing CO2 (5.0%). After the medium removal, each well received enough SFE (40 °C/30 MPa) to reach the desired concentration (1; 10; 100 or 1,000 µg/ml) using supplemented DMEM. SFE were previously solubilized with DMSO (0.1%) (Lemaire et al., 2011) and treatment lasted 24 or 48 h. Then, after 2 h for incubation with tetrazolium salt, the cell viability was verified through cytotoxicity MTT assay (Mosmann, 1983). Absorbance readings at 540 nm allowed to IC50 calculations.

Effects of treatments with SFE in colony proliferation was accessed using breast cancer cells (MCF-7; 500 cells/well; 6 well/plate) that were kept overnight for adherence. Then, cells were submitted to SFE treatment done with non-cytotoxic concentrations (10 or 20 µg/ml), during 24 h (Franken et al., 2006). Negative control received DMSO (0.1%) solubilized in supplemented DMEM, as mentioned before. Thus, after washed with PBS, the cells were kept in supplemented DMEM for recovery for 20 days. At the end of this period, all colonies were stained with crystal violet (0.5%). Image J version 1.49 software (National Institute of Health, Bethesda, MD, USA) allowed counting the colonies through digital images.

The type of cell death was evaluated with confluent MCF-7 cells (2×10^5 cells/well; 6 wells plate). These cells received treatment with SFE at 10 or 20 µg/ml, during 24 h. Cells exposed to DMSO (0.1%) were

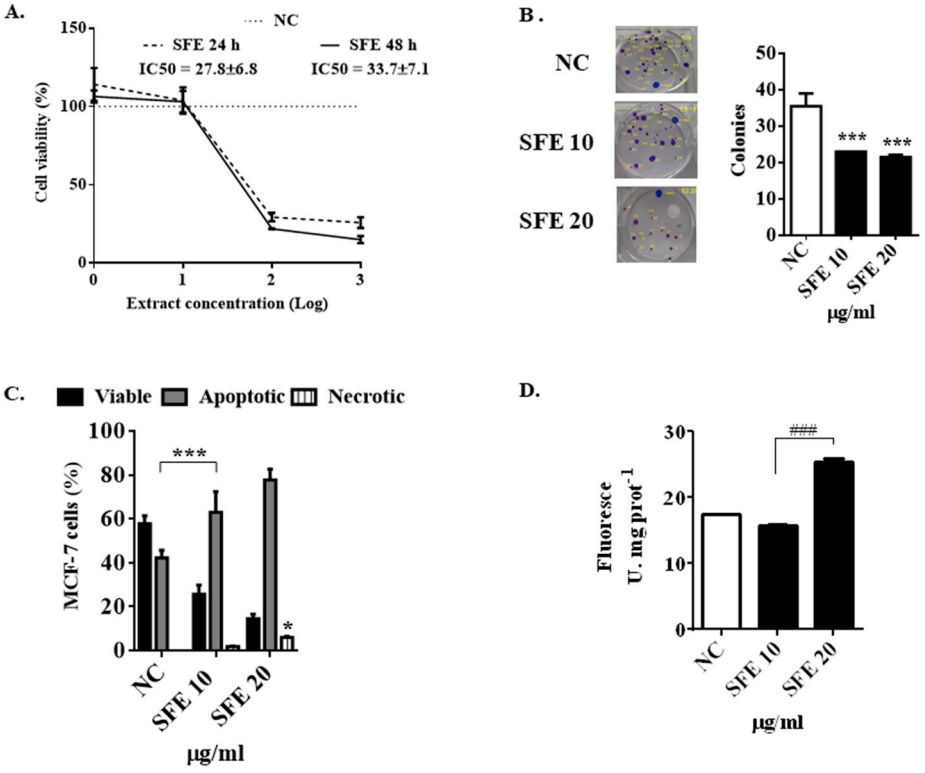

Fig. 1. Cytotoxic effects of *Piper nigrum* SFE 40 °C/30 MPa (1–1000 µg/ml; 24 and 48 h) in MCF-7 cells were observed through MTT assay (A). Clonogenic assay revealed SFE treatment (24 h) decreased number of colonies observed after recovery time (20 days) (B). Types of cell death induced after treatment with SFE during 24 h (C). * and *** denote statistical differences compared to negative control (NC) when $p < 0.05$ and $p < 0.001$, respectively.

negative control. Then, after trypsinized and washed (PBS) the cells were centrifuged (1,000 rpm/5 min) and the obtained pellet was suspended with PBS. Apoptosis or necrosis were verified through fluorescence of propidium iodide (100 µl/ml) plus acridine orange (100 µl/ml) (1:1; v/v). Then, up to 300 cells/glass slide were counted, twice. Results showed percentage of viable, apoptotic or necrotic cells (McGahon et al., 1995).

2.5. In vivo tumor growth evaluation

2.5.1. Animals, tumor induction and treatment

Isogenic Balb/c mice were housed and received treatments accordingly with legal requirements (NIH publication #80–23, revised in 1978) and local Ethics Committee for Animals Use approved protocol (CEUA/UFSC PPOO784). Preliminary studies determined the maximum tolerated dose of SFE 40 °C/30 MPa (10; 50; 100 and 150 mg/kg/day) (data not shown). Recognition of pain and distress signs linked with behavior (lethargy, tremors); physical signs (altered respiration rates; dullness of eyes); piloerection, hair loss and changes in food and water consumption were used as exclusion criteria. Higher dose (150 mg/kg) tested caused death (data not shown) and best results achieved was using 100 mg/kg/day. Thus, all next experiments were comparatively conducted only which the lower (10 mg/kg/day) and the higher tested dose (100 mg/kg/day). Briefly, mice (male; 65 days old; 21.0 ± 1.0 g) abdominal circumference and weight were measured and inoculated intraperitoneally with Ehrlich ascites carcinoma cells (EAC) (200 µl; 5×10^6 cells/mice) (Kviecinski et al., 2011). Treatments were initiated 24 h after EAC inoculation and were extended for 9 consecutive days. Four experimental groups (n = 16) received intraperitoneally the same volume of treatment (50 µl). Two groups received doses of SFE 40 °C/30 MPa (100 mg/kg/day or 10 mg/kg/day solubilized firstly in Tween 80, 1.0% and subsequently in saline NaCl; 0.8%). Positive control group received Doxorubicin (1.2 mg/kg/day). Negative control group received saline (NaCl; 0.8%) prepared with Tween 80 (1.0%). Then, 24 h after the last treatment mice (n = 6) of each group were euthanized and EAC was collected for cytological and biochemical determinations. At same time mice (n = 10) from each treatment were randomly chosen and kept alive to verify the effects of SFE in the survival time using Kaplan-Meier curve (Kaplan and Meier, 1958) and these evaluations were interrupted after 30 days.

2.5.2. EAC cell cycle and type of death induced by black pepper SFE

Tumor cells were collected from mice-bearing Ehrlich ascites carcinoma cells (EAC). Then, EAC cells cycle effects were evaluated with propidium iodide/RNAse solution kit, applying protocol proposed by the manufacturer (Immunostep; Salamanca, Spain). EAC from mice of all groups (4×10^5 cells/ml) were washed with PBS, fixed overnight (ethanol 70%) and kept at −20 °C. After thawing and another wash in PBS, each pellet was gently suspended in the solution of propidium iodide/RNAse followed by incubation during 15 min at room temperature. Then, cell cycle effects were determined through readings of 10,000 events in the BDFACS Canto II flow cytometer (BD Biosciences) which used Flowing Software version 2.5.1 (Turku, Finland).

Additionally, studies were conducted to verify the type of death induced in Ehrlich ascites carcinoma cells (EAC) after *in vivo* treatment done as described previously. Briefly, EAC cells were collect from mice, washed with NaCl (0.8%) (10 min; 1,000 rpm). Then, EAC cells (5×10^6 cells) were stained with ethidium bromide (100 µg/ml) and acridine orange (100 µg/ml) (5 µl; 1:1; v/v). Three hundred EAC cells by each glass slide were visualized under fluorescence microscopy. The results from three slides showed the percentage of viable (green), apoptotic (orange) or necrotic (red) cells (McGahon et al., 1995). Positive control received Doxorubicin (0.2 mg/kg/day) which allowed EAC cells proliferation.

2.5.3. Western blotting protein analysis

Immunoblotting assays made possible to detect levels of protein level related to DNA damage (p53), cell cycle progression (CDK2 and Cyclin A) and apoptosis induction (Bax) or apoptosis inhibition (Bcl-xL). Therefore, EAC cells (5 × 106) were collected from mice, washed with PBS and lysed with RIPA buffer (Tris–HCl, 50 mM, pH 7.4; NaCl, 150 mM; Nonidet P-40 solution, 1.0%; Na-deoxycholate, 0.25% and

Table 1
In silico assay, docking features related to interactions between piperine (PubChem CID 638024) and protein CDK2-cyclin A-Peptide substrate complex (PB 1QMZ). Intermolecular contributions predicted by AutoDock Vina Score One Function.

CDK2-Cyclin A (PDB 1QMZ)

Search box centre (size x=y=z; Å)	Piperine Position	Affinity energy (kcal/mol)	RMSD	Hydrophobic Interactions	Hydrogen bonding	Residues of CDK2-Cyclin A bonded with PIP
ATP binding site Chain A (25)	L1	-8.17885	0.000	47.96261	0.75431	Lys^{89}: Chain A
	L2	-8.08008	2.823	53.97527	0.59771	Gln^{85}: Chain A
	L4	-7.86405	2.053	50.99747	0.00000	-
Lys^{8} Chain E (30)	L1	-7.86437	0.000	29.62868	0.42211	-
	L2	-7.62061	3.35	34.32364	0.90516	Ser^{5}: Chain E

A. PIP L1 - Box centered at ATP binding site

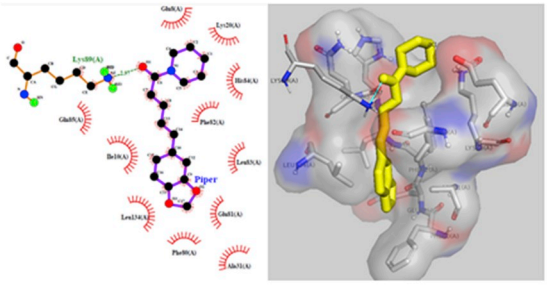

B. PIP L2 - Box centered at Lys^{8} Chain E

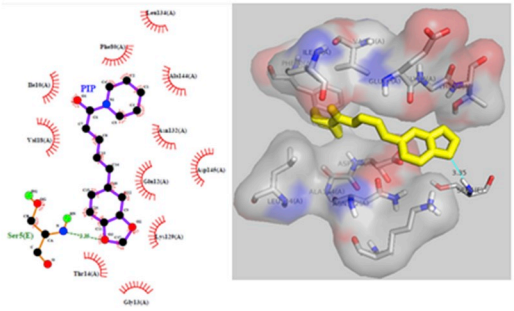

Inserts A&B- Diagram of piperine (PIP) (PubChem CID 638024) poses interacting with CDK2-Cyclin A amino acids as predicted by AutoDock Vina. LigPlot^{+} predicted hydrophobic interactions are shown as solid red lines, hydrogen bonds are shown as dashed green lines, and calculated distances are indicated. Protein side chains that do not interact with ligand have been omitted from the figure. Binding site was depicted with sticks and molecular surface using PyMol version 1.8.x Open Source (2015-12-22). PIP L1 - Box centered at ATP binding site (insert A); PIP L2 - Box centered at Lys^{8} Chain E (insert B).

phenylmethylsulfonyl fluoride, 1 mM) supplemented with protease (1.0%) and phosphatase cocktail (3.0%) inhibitors kept enzymes phosphorylated. Protein were denatured with Laemmli buffer (Tris-HCl, 60 mM, sodium dodecyl sulfate, 2%; glycerol l0%; β-mercaptoethanol 5%; bromophenol blue, 0.01%; pH 6.8) and quantified (Bradford, 1976). Then, protein (30 ng) separated by electrophoresis using SDS-PAGE with acrylamide (10%) and transferred to PVDF membranes. Non-specific interactions in membranes were blocked using non-fat milk solubilized with buffer Tris-NaCl (60 mM) and Tween 20 (0.1%) (pH 7.6). Membranes were exposed (overnight) to primary antibodies and washed three times using the same buffer. Then, exposed during 2 h to secondary antibodies conjugated with peroxidase. Finally, immunoreactive proteins were visualized using ChemiDoc MP System (Bio Rad) and normalized by actin. Loading control used was actin (Laemmli, 1970; Dejeans et al., 2010).

2.6. Statistical analysis

In vitro assays results come from three independent experiments performed in triplicates and expressed as means ± standard deviation. ANOVA test followed by Dunnett's test allowed to analyze data processed using the GraphPad Prism version 6.0 software (San Diego, USA). Values of $p < 0.05$ were statistically significant.

3. Results and discussion

Supercritical carbon dioxide extraction has solvent power modulation capabilities with enhanced selectivity making higher quality fractioned extracts from natural matter (Ciftci, 2012). Indeed, piperine was the major secondary metabolite (49.24 ± 0.02%) identified in the extract obtained by SFE at 30 MPa bar and 40 °C (Grinevicius et al., 2017). Piperine or 1-piperoylpiperidine piperine (molecular formula $C_{17}H_{19}NO_3$) (PubChem CID: 638024) can enhance bioavailability of other phytochemicals through mechanisms including increasing their absorption and modulation of their metabolism (Kakarala et al., 2010).

3.1. Molecular docking predicts piperine interaction with CDK2 and Bcl-xL

Docking simulations done with CDK2-cyclin A-Peptide substrate complex (PDB 1QMZ) search space for docking was set up using amino acid residues at chain A (Glu^{81}; Leu^{83}; Lys^{89}) and chain E (Ser^{5}). These residues correspond to ATP binding site (Brown et al., 1999). Besides, another search space for docking was centered in the amino acid residue Lys^{8}. This residue kept peptide substrate linked to cyclin A through a hydrogen bond (Brown et al., 1999). Such interactions, predicted by AutoDock Vina, included hydrophobic interactions observed in the 2D diagram generated with LigPlot^{+}. These interactions were visualized with PyMOL version 1.8. x Open Source using as template the structure of PDB 1QMZ (Fig. 1 S A).

Table 2
In silico assay, docking features related to interactions between piperine (PubChem CID 638024) and protein Bcl-xL (PDB 4TUH) chain A inside inhibitor site. Intermolecular contributions predicted by AutoDock Vina Score One Function.2

Bcl-xL (PDB 4TUH)						
Search box centre (size x=y=z; Å)	Piperine Position	Affinity energy (kcal/mol)	RMSD	Hydrophobic interactions	Hydrogen bonding	Residues of Bcl-xL (Chain A) bonded with PIP
Inhibitor binding site Chain A (25)	L1	-10.1	0.000	72.83550	0.79774	Arg^{139}
	L2	-9.8	1.802	74.03226	0.56587	-
	L3	-9.6	2.844	89.05603	1.03148	Leu^{108}
	L4	-9.2	6.751	84.43719	0.42065	Arg^{139}

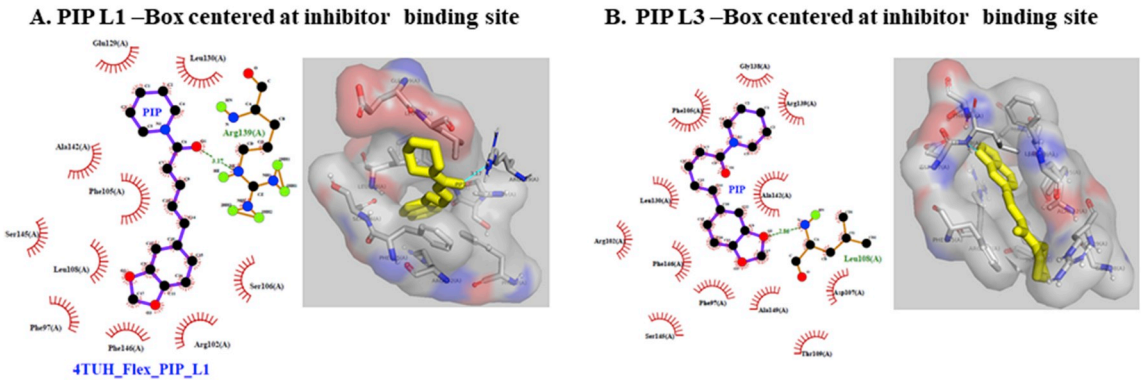

Inserts A&B- Diagram of piperine (PIP) (PubChem CID 638024) poses interacting with Bcl-xL amino acids as predicted by AutoDock Vina. LigPlot$^+$ predicted hydrophobic interactions are shown as solid red lines, hydrogen bonds are shown as dashed green lines, and calculated distances are indicated. Protein side chains that do not interact with ligand have been omitted from the figure. Binding site was depicted with sticks and molecular surface using PyMol version 1.8.x Open Source (2015-12-22). Search space (Grid box) were centered at inhibitor binding site inside hydrophobic groove of Bcl-xL.

Hydrogen bonds were formed when a hydrogen atom interact with a strong electronegative atom like N, O or F inside the macromolecule structure. Interactions calculated with AutoDock Vina predicted nitrogen-oxygen hydrogen bonds and hydrophobic interactions between piperine and residues positioned at chain A (CDK2) and chain E (peptide substrate). Piperine predicted pose L1 at ATP binding site (RMSD = 0.000) had lowest affinity binding energy (−8.2 kcal/mol) and showed one H-bond between piperine oxygen atom (O1) and nitrogen atom of CDK2 residue Lys^{89}. Piperine at pose L1 also had hydrophobic interactions (47.96261) with CDK2 residues including Leu^{83} inside chain A (Table 1, insert A). Additionally, piperine at pose L2 (RMSD = 2.823) had oxygen H-bounded with nitrogen (residue Gln^{85}) and highest hydrophobic predicted interactions (53.99747). It is important to highlight that residues Lys^{89} and Leu^{83} have hydrogen bonds with ATP inside structure of crystallized protein used as template (PDB 1QMZ) (Brown et al., 1999).

Table 1 also shows predicted best pose of piperine when docked using search box positioned at ATP binding site or centered at residue Lys^{8}, which kept peptide substrate hydrogen, bonded with cyclin A. Docking results using search box centered at Lys^{8} (chain E; PDB 1QMZ) showed hydrophobic interactions (34.32364). Besides, docking simulation predicted one H-bond between oxygen and nitrogen molecules present in the methylenedioxyphenyl moiety of piperine (pose L2) (RMSD = 3.35) and phosphorylatable serine residue (Ser^{5}) inside peptide substrate (chain E) with favorable affinity energy (−7.62061) (Table 1, insert B). This residue is the binding site of ATP molecule inside phosphorylated complex (CDK2-cyclin A-Peptide substrate) (PDB 1QMZ). Predicted poses of piperine suggest that it could be occupying ATP binding site and, consequently impeding the phosphorylation necessary to activate CDK2-Cyclin A heterodimer (Jacobsen et al., 2012). Moreover, AutoDock Vina scoring function allowed predicting how strongly each docked pose of such putative ligand binds to the target protein (Li et al., 2015). These docking simulations results could be predictive of piperine inhibitory activity.

The second target protein was Bcl-xL (PDB 4TUH), which was submitted to AutoDock Tools preparations before docking. The search space used for docking simulations included Bcl-xL binding site amino acid residues (Leu^{108}, Ser^{106} and Asn^{136}) occupied for its inhibitor (Koehler et al., 2014). Preliminary LigPlot$^+$ analysis was restricted to protein PDB 4TUH chain A containing inhibitor structure. Diagrams generated showed hydrogen bonds formed between inhibitor and protein at residues Ser^{106}, Leu^{108}, Asn^{136} and Arg^{139}. LigPlot$^+$ generated diagram also showed inside inhibitor-protein complex several hydrophobic interactions at residues Ala^{93}; Glu^{96}; Phe^{97}; Tyr^{101}; Arg^{102}; $Pheo^{105}$; Ser^{106}; Asp^{107}; Leu^{108}; Thr^{109}; Glu^{129}; Leu^{130}; Asn^{136}; Gly^{138}; Arg^{139} Ala^{142}; Ser^{145}; Phe^{146} and Tyr^{195} keeping inhibitor inside the chain A hydrophobic groove in the crystalized Bcl-xL template (PDB 4TUH) (Fig. 1 S B).

Thus, in order to find out what residues inside Bcl-xL inhibitor hydrophobic groove could further interact with piperine other investigations with LigPlot$^+$ were done using PDB format data from PDB 4TUH (Koehler et al., 2014). AutoDock Vina predicted the best favorable binding affinity for flexible ligand piperine at pose L1 (−10.1 kcal/mol) (Table 2, insert A) and pose L3 (−9.7 kcal/mol) (Table 2, insert B).

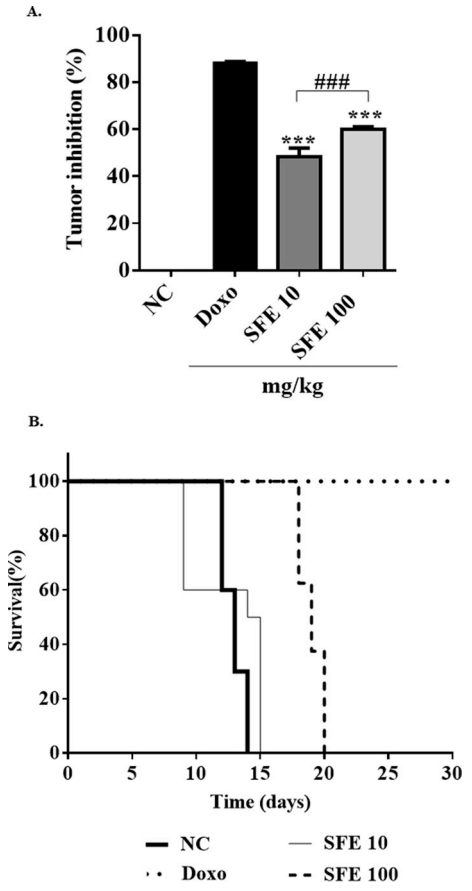

Fig. 2. *In vivo* assays with Balb/c mice bearing EAC (male; 65 days old; 21.0 ± 1.0 g body weight) treated intraperitoneally with *Piper nigrum* SFE 40 °C/30 MPa (10 or 100 mg/kg/day; 9 days). SFE inhibited EAC growth (A). SFE increased mice survival (B). *** denotes statistical difference comparatively to negative control (NC) and ### denotes statistical difference compared to positive control (Doxo), when $p < 0.001$.

AutoDock Vina score one function also predicted interactions for piperine inside the hydrophobic groove of this protein. Piperine had hydrophobic interactions at pose L1 (72.83550) lower than at pose L3 (89.5603). Piperine at pose L3 interact with higher number of nonpolar amino acids comparatively to pose L1 (Table 2 insert B).

Inside Bcl-xL binding grove piperine docked at pose L1 and L3 (Table 2 insert B) showed H-bonds with residues Arg^{139} and Leu^{108}, respectively. These interactions were visualized with LigPlot$^+$ (2D) and PyMOL version 1.8. x Open Source (3D) using structure of PDB 4TUH, as template. Besides, the amphipathic character of piperine stablished hydrophobic interactions inside the hydrophobic pocket of Bcl-xL (chain A). Surprisingly, piperine had hydrophobic interactions with practically all residues of binding site occupied by Bcl-xL inhibitor (Table 2 inserts A and B). These findings suggest probable inhibitory interactions of piperine with anti-apoptotic protein Bcl-xL, because it was demonstrated that molecular docking results predicted piperine (pose L1 and L3) (Table 2 inserts A and B) interacted with residues located in the same binding site occupied by the inhibitor of Bcl-xL (PDB 4TUH), showed as supplementary material (Fig. S1 B).

3.2. Black pepper SFE inhibited the growth of breast cancer cell line MCF-7

The cytotoxic effects of SFE against MCF-7 cells were observed through MTT assay. The calculated value of SFE inhibitory concentration (IC_{50}) was indicative of cytotoxicity after 24 h (IC_{50} = 27.8 ± 6.8 µg/ml) and after 48 h (IC_{50} = 33.7 ± 6.8 µg/ml), with no statistical differences (Fig. 1 A). Thus, the *in vitro* clonogenic assays were carried out only with 24 h of treatment.

Clonogenic assays revealed significant decreased number of colonies observed after a recovery time of twenty days counted after the end of the period of treatment with non-cytotoxic concentrations of SFE (10 or 20 µg/ml; 24 h). Results showed significant reduction in the number of colonies for both SFE treatments ($p < 0.001$), comparatively to negative control (Fig. 1 B). Thereby, few remaining cells were able to surpass the cytotoxic effect and grew up. As mentioned before, the MTT assay showed SFE sample capability to cause cell cytotoxicity triggering cell death. Further investigations showed that the SFE treatment increased the number of apoptotic cells ($p < 0.001$), comparatively to negative control (Fig. 1 C), although that cells number under necrosis were significantly higher after treatment with 20 µg/ml ($p < 0.01$), comparatively to controls.

Meanwhile, synergism among piperine and other extracted phytocompounds could result in the observed anti-tumor activity. Indeed, black pepper ethanolic extract with higher content of piperine and terpenes caused more cytotoxicity and had anti-proliferative effects

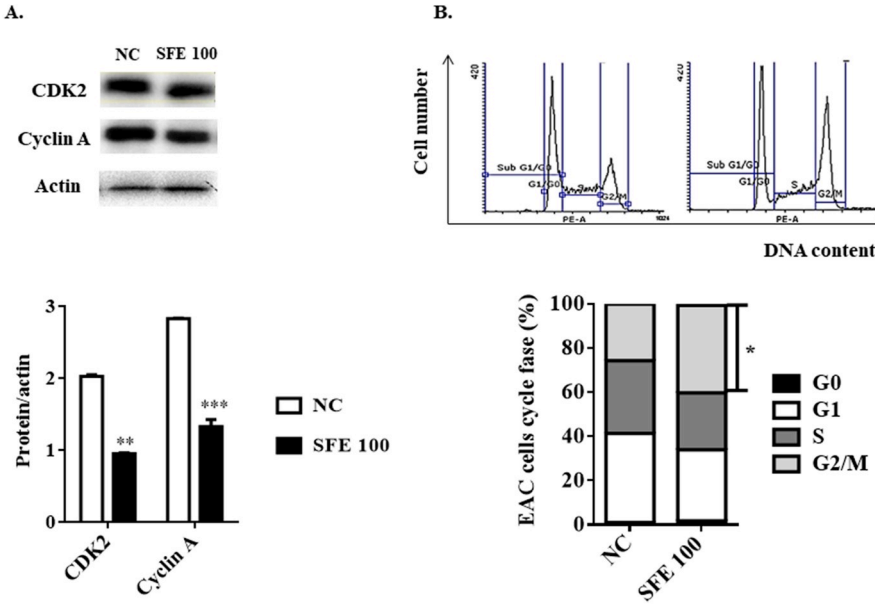

Fig. 3. Treatments done with *Piper nigrum* SFE 40 °C/30 MPa (100 mg/kg/day; 9 days) inhibited expression of CDK2 and cyclin A of EAC collected from EAC-bearing mice (A). SFE caused EAC cell cycle arrest at G2/M (B). *; ** and *** denote statistical differences comparatively to negative control (NC) when $p < 0.05$; $p < 0.01$ and $p < 0.001$, respectively.

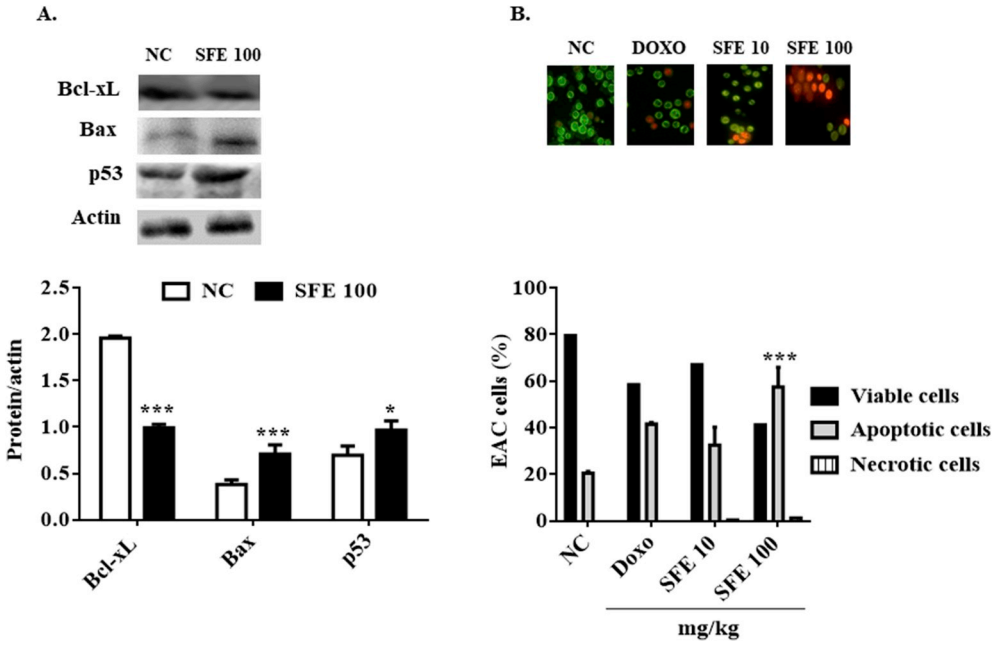

Fig. 4. Treatments done with *Piper nigrum* SFE 40 °C/30 MPa (100 mg/kg/day; 9 days) inhibited antiapoptotic protein Bcl-xL expression of EAC collected from EAC-bearing mice and increased expression of apoptotic proteins Bax and p53 (A). Positive control done with Doxorubicin (0.2 mg/kg) and SFE enhanced the number of apoptotic deaths of EAC (B). * and *** denote statistical differences compared with negative control (NC) when $p < 0.05$ and $p < 0.001$, respectively.

against MCF-7 cells (Grinevicius et al., 2016). Piperine showed *in vitro* anti-tumor activity and anti-proliferative activity against other breast cancer cells (Do et al., 2013). Therefore, piperine presence in SFE could partially justify some of inhibitory effects observed. These results also corroborate the theoretical data obtained with CDK2 - cyclin A docking. The simulation predicted H-bond formation between piperine and CDK2 at ATP binding site, which could have interrupted the cell cycle, inhibited cell proliferation and contributed to apoptotic cell death as observed previously with MCF-7 cells (Fig. 1 C). Piperine treatments inhibited expression of DNA polymerase beta of melanoma cells (Fofaria et al., 2014).

3.3. Black pepper SFE inhibited EAC tumor growth

This *in vivo* study intended to corroborate the cytotoxicity of SFE and its antiproliferative potential observed *in vitro*. Data from EAC-bearing mice showed tumor inhibition (Fig. 2 A) and treatment done at 100 mg/kg increased significantly the tumor inhibition (60%) ($p < 0.01$) and also increased the survival of mice (33%) comparatively to the group that received lower dose (Fig. 2 B). Besides, treatment done with SFE (100 mg/kg/day) achieved 50% of survival values compared to positive control and positive control was carried out with Doxorubicin (1.2 mg/kg/day) which inhibited completely the growth of the tumor and were considered as 100% of survival.

3.4. Black pepper SFE induced cancer cells apoptosis and cycle arrest correlated with proteins level

EAC tumor cells were used to immunoblotting, which showed reduced level of CDK2 and cyclin A (Fig. 3 A). Cells cycle progression are ruled by cyclin dependent kinases which are activated at specific point during cell cycle and targeted to its substrates in proper cellular regions (Brown et al., 1999). Besides, expression of distinct CDK-cyclin complexes vary accordingly to each phase during cell cycle progression and CDK2-cyclin A is active during S phase.

Nevertheless, comparatively to negative control where these protein levels were at least two-fold higher, mice bearing-EAC treated with SFE (100 mg/kg/day) showed significant lower levels of CDK2 ($p < 0.01$) and cyclin A ($p < 0.001$). Thus, decreased expression of CDK2 and cyclin A contributed to inhibit EAC tumor growth (Fig. 2 A) confirming docking simulations. Docking findings (Tables 1 and 2) could partially explain variations in EAC protein activity and perhaps their expression and caused EAC cell cycle effects after the mice were treated with SFE (100 mg/kg/day).

Bioactive phytocompounds isolated from herbs including piperine inhibited cancer cells growth, which were observed through *in vivo* experiments done with Swiss mice transplanted with sarcoma 180 cells. Mice received intraperitoneally piperine (50 mg/kg/day or 100 mg/kg/day) for 7 days and both treatments inhibited solid tumor up to 55 and 57%, respectively (Bezerra et al., 2006). Piperine positioned at residue Lys^8 can inhibit heterodimer formation while piperine positioned at ATP binding site can inhibit phosphorylation of CDK2 - cyclin A. Since both are necessary to cell cycle progress through the different phases of synthesis (S) (Jacobsen et al., 2012), consequently less EAC reaches the S phase as shown in Fig. 3 B.

The inhibited expression of cyclin A was verified through immunoblotting, which also represents a bottleneck to cell cycle leaves G1, because cyclin A appropriate level is necessary to cell cycle progress (Luciani et al., 2000). It was demonstrated here that treatments with SFE 100 mg/kg showed a slight decreased in phase G1 (20.6%) and phase S (22.6%) and significant increased phase G2/M ($p < 0.05$) (51.4%) (Fig. 3 B). Piperine exerted growth-inhibitory effects correlated with cytotoxicity and antiproliferative activity and cell cycle impairment via G2/M phase arrest through increased apoptosis of human oral squamous carcinoma cells (Siddiqui et al., 2017), osteosarcoma cells (Zhang et al., 2015), lung cancer cells (Lin et al., 2014), as well as in liver cancer cells (Gunasekaran et al., 2017).

After SFE treatment (100 mg/kg/day) of mice-bearing EAC, the tumor cells were collected and immunoblotting, showing increased level of pro-apoptotic Bax ($p < 0.001$) and decreased expression of anti-apoptotic protein (Bcl-xL) ($p < 0.001$), comparatively to negative control (Fig. 4 A). Results showed expression of p53 were slightly higher comparatively to controls ($p < 0.05$) (Fig. 4 A). Tumor suppressor p53 is a negative regulator of the cell cycle and upon DNA damage can delay or arrest cells at G1/S checkpoint preceding DNA replication (phase S) (Lavin and Gueven, 2006). The study with tumor suppressor p53 showed that the DNA binding region of p53 can cause structural alterations in Bcl-xL, thereby facilitating interactions with BH3-only proteins (Hagn et al., 2010). Therefore, BH3-only proteins displace Bax complexed with anti-apoptotic protein Bcl-xL and these formed Bax monomers promotes apoptosis signaling through mitochondrial membrane permeabilization. It was demonstrated that

increased p53 levels induced apoptosis via p53-dependent mitochondrial signaling pathway (Lin et al., 2014).

EAC cells collected from EAC-bearing mice treated with SFE (100 mg/kg/day) fraction rich in piperine showed a significant increased number of apoptotic cells ($p < 0.001$) when compared to negative control (Fig. 4 B). Piperine also induced apoptosis against melanoma and rectal cancer cells (Fofaria et al., 2014). Multiple signaling pathways related to cell cycle arrest and apoptosis of cancer cells can be restrained through piperine modulation (Lu et al., 2012).

4. Conclusions

This study showed phytocompounds from *Piper nigrum* L. cultivar Bragantina recovered by supercritical carbon dioxide extraction, a green technology. The cytotoxicity, anti-proliferative and anti-tumor activities of SFE occurred probably due to synergism between phytocompounds and piperine extracted from black pepper. Protein inhibition were confirmed through low levels of cell cycle control proteins CDK2 and cyclin A and anti-apoptotic protein Bcl-xL. Besides, experimental data can be aligned with theoretical *in silico* approach applied to predict molecular interactions between piperine and target proteins.

Conflicts of interest

The authors declare no conflict of interest.

Declaration of interest

The authors declare that they have no known competing financial interests or personal relationships that could have appeared to influence the work reported in this paper.

Acknowledgments

This research was supported by scholarships granted to researchers by CNPq (Brazilian National Research Council) and CAPES (Coordination of Superior Level Staff Improvement) and scholarships granted for post doc by CAPES/PNPD/PPGFAR UFSC. This research was supported by grants from Conselho Nacional de Pesquisa (CNPq) and from Coordenação de Aperfeiçoamento de Pessoal de Nível Superior Brazil. RCP (Proc. 302404/2017–2) and S.R.S.F are recipients of research grants from CNPq, Brazil. RCZ, NSRSM, K.S.A and VMASG are fellows of CAPES/CNPq, Brazil.

Appendix A. Supplementary data

Supplementary data to this article can be found online at https://doi.org/10.1016/j.fct.2019.110644.

References

Andrade, K.S., Trivellin, G., Ferreira, S.R.S., 2017. Piperine-rich extracts obtained by high pressure methods. J. Supercrit. Fluids 128, 370–377.

Attard, T.M., McElroy, C.R., Hunt, A.J., 2015. Economic assessment of supercritical CO2 extraction of waxes as part of a maize stover biorefinery. Int. J. Mol. Sci. 16, 17546–17564. https://doi.org/10.3390/ijms160817546.

Bertini, I., Chevance, S., Del Conte, R., Lalli, D., Turano, P., 2011. The anti-apoptotic bcl-xl protein, a new piece in the puzzle of cytochrome C interactome. PLoS One 6, e18329.

Bezerra, D.P., Castro, F.O., Alves, A.P.N.N., Pessoa, C., Moraes, M.O., Silveira, E.R., Lima, M.A.S., Elmiro, F.J.M., Costa-Lotufo, L.V., 2006. In vivo growth-inhibition of Sarcoma 180 by piplartine and piperine, two alkaloid amides from piper. Braz. J. Med. Biol. Res. 39, 801–807.

Bradford, M.M., 1976. A rapid and sensitive method for the quantitation of microgram quantities of protein utilizing the principle of protein dye binding. Anal. Biochem. 72, 248–254.

Brown, N.R., Noble, M.E.M., Endicott, J.A., Johnson, L.N., 1999. The structural basis for specificity of substrate and recruitment peptides for cyclin-dependent kinases. Nat. Cell Biol. 1, 438–443.

Chaveerach, A., Mokkamul, P., Sudmoon, R., Tanee, T., 2006. Ethnobotany of the genus piper (piperaceae) in Thailand. Ethnobot. Res. Appl. 4, 223–231.

Chemat, F., Vian, M.A., Cravotto, G., 2012. Green extraction of natural products: concept and principles. Int. J. Mol. Sci. 13, 8615–8627.

Ciftci, O.N., 2012. Supercritical fluid technology: application to food processing. J. Food Process. Technol. 3, e105. https://doi.org/10.4172/2157-7110.1000e105.

Clarke, T.C., Black, L.I., Stussman, B.J., Barnes, P.M., Nahin, R.L., 2015. Trends in the use of complementary health approaches among adults: United States 2002-2012. Natl. Health Stat Report. 79, 1–16.

Dejeans, N., Tajeddine, N., Beck, R., Verrax, J., Taper, H., Gailly, P., Calderon, P.B., 2010. Endoplasmic reticulum calcium release potentiates the ER stress and cell death caused by an oxidative stress in MCF-7 cells. Biochem. Pharmacol. 79, 1221–1230.

Do, M.T., Kim, H.G., Choi, J.H., Khanal, T., Park, B.H., Tran, T.P., Jeong, T.C., Jeong, H.G., 2013. Antitumor efficacy of piperine in the treatment of human HER2-over-expressing breast cancer cells. Food Chem. 141, 2591–2599.

Fofaria, N.M., Kim, S.H., Srivastava, S.K., 2014. Piperine causes G1 phase cell cycle arrest and apoptosis in melanoma cells through checkpoint kinase-1 activation. PLoS One 9 (5), e94298. https://doi.org/10.1371/journal.pone.0094298.

Forlemu, N., Watkins, P., Sloop, J., 2017. Sulfonamide derivatives as potential anti-malarial agents targeting the glycolytic enzymes: GAPDH, aldolase and TPI. Open J. Biophys. 7, 41–57.

Forli, S., Huey, R., Pique, M.E., Sanner, M., Goodsell, D.S., Olson, A.J., 2016. Computational protein-ligand docking and virtual drug screening with the AutoDock suite. Nat. Protoc. 11 (5), 905–919.

Franken, N.A.P., Rodermond, H.M., Stap, J., Haveman, J., Chris van Bree, C., 2006. Clonogenic assay of cells in vitro. Nat. Protoc. 1, 2315–2319.

Grinevicius, V.M.A.S., Andrade, K.S., Ourique, F., Micke, G.A., Ferreira, S.R.S., Pedrosa, R.C., 2017. Antitumor activity of conventional and supercritical extracts from *Piper nigrum* L. cultivar Bragantina through cell cycle arrest and apoptosis induction. J. Supercrit. Fluids 128, 94–101.

Grinevicius, V.M.A.S., Kviecinski, M.R., Mota, N.S.R.S., Ourique, F., Castro, L.S.E.P.W., Andreguetti, R.R., Correia, J.F.G., Wilhelm Filho, D., Pich, K.T., Pedrosa, R.C., 2016. *Piper nigrum* ethanolic extract rich in piperamides causes ROS overproduction, oxidative damage in DNA leading to cell cycle arrest and apoptosis in cancer cells. J. Ethnopharmacol. 189, 139–147.

Gunasekaran, V., Elangovan, K., Devaraj, S.N., 2017. Targeting hepatocellular carcinoma with piperine by radical-mediated mitochondrial pathway of apoptosis: an *in vitro* and *in vivo* study. Food Chem. Toxicol. 105, 106–118.

Hagn, F., Klein, C., Demmer, O., Marchenko, N., Vaseva, A., Moll, U.M., Kessler, H., 2010. Bcl-xL changes conformation upon binding to wild-type but not mutant p53 DNA binding domain. J. Biol. Chem. 285 (5), 3439–3450.

Jacobsen, D.M., Bao, Z.Q., O'Brien, P., Brooks III, C.L., Young, M.A., 2012. Price to Be paid for two-metal catalysis: magnesium ions that accelerate chemistry unavoidably limit product release from a protein kinase. J. Food Process. Technol. 134 (37), 15357–15370.

Kakarala, M., Brenner, D.E., Khorkaya, H., Cheng, C., Tazi, K., Ginestier, C., Liu, S., Dontu, G., Wicha, M.S., 2010. Targeting breast stem cells with the cancer preventive compounds curcumin and piperine. Breast Canc. Res. Treat. 122 (3), 777–785.

Kaplan, E.L., Meier, P., 1958. Nonparametric estimation from incomplete observations. J. Am. Stat. Assoc. 53 (282), 457–481.

Koehler, M.F., Bergeron, P., Choo, E.F., Lau, K., Ndubaku, C., Dudley, D., Gibbons, P., Sleebs, B.E., Rye, C.S., Nikolakopoulos, G., Bui, C., Kulasegaram, S., Kersten, W.J.A., Smith, B.J., Czabotar, P.E., Colman, P.M., Huang, D.C.S., Baell, J.B., Watson, K.G., Hasvold, L., Tao, Z.F., Wang, L., Souers, A.J., Elmore, S.W., Flygare, J.A., Fairbrother, W.J., Lessene, G., 2014. Structure-guided rescaffolding of selective antagonists of Bcl-xL. ACS Med. Chem. Lett. 5, 662–667.

Kurian, J.C., 2012. Ethno-medicinal plants of India, Thailand and vietnam. J. Biodivers. 3 (1), 61–75.

Kviecinski, M.R., Benelli, P., Felipe, K.B., Correia, J.F.G., Pich, C.T., Ferreira, S.R.S., Pedrosa, R.C., 2011. SFE from *Bidens pilosa* Linné to obtain extracts rich in cytotoxic polyacetylenes with antitumor activity. J. Supercrit. Fluids 56, 243–248.

Laemmli, U.K., 1970. Cleavage of structural protein during assembly of the head of bacteriophage T4. Nature 227, 680–685.

Lai, L.H., Fu, Q.H., Liu, Y., Jiang, K., Guo, Q.M., Chen, Q.Y., Yan, B., Wang, Q.Q., Shen, J.G., 2012. Piperine suppresses tumor growth and metastasis *in vitro* and *in vivo* in a 4T1 murine breast cancer model. Acta Pharmacol. Sin. 33, 523–530.

Laskowski, R.A., Swindells, M.B., 2011. LigPlot^{+}: multiple ligand-protein interaction diagrams for drug discovery. J. Chem. Inf. Model. 51 (10), 2778–2786.

Lavin, M.F., Gueven, N., 2006. The complexity of p53 stabilization and activation. Cell Death Differ. 13, 941–950.

Lemaire, B., Beck, M., Jaspart, M., Debier, C., Calderon, P.B., Thomé, J.P., Rees, J.F., 2011. Precision-cut liver slices of *Salmo salar* as a tool to investigate the oxidative impact of CYP1A-mediated PCB 126 and 3-methylcholanthrene metabolism. Toxicol. Vitro 25 (1), 335–342.

Liao, G.S., Apaya, M.K., Shyur, L.F., 2013. Herbal medicine and acupuncture for breast cancer palliative care and adjuvant therapy. Evid. Based Complement Altern. Med. 17. https://doi.org/10.1155/2013/437948. Article ID 437948.

Li, H., Leung, K.S., Wong, M.H., Ballester, P.J., 2015. Improving AutoDock Vina using Random Forest: the growing accuracy of binding affinity prediction by the effective exploitation of larger data sets. Mol. Inform. 34 (2–3), 115–126.

Lin, Y., Xu, J., Liao, H., Li, L., Pan, L., 2014. Piperine induces apoptosis of lung cancer A549 cells via p53-dependent mitochondrial signaling pathway. Tumour Biol. 35, 3305–3310 (2014).

Luciani, M.G., Hutchins, J.R.A., Zheleva, D., Hupp, T.R., 2000. The C-terminal regulatory domain of p53 contains a functional docking site for cyclin A. J. Mol. Biol. 300, 503–518.

Lu, J.J., Bao, J.L., Chen, X.P., Huang, M., Wang, Y.T., 2012. Alkaloids isolated from

natural herbs as the anticancer agents. Evid. Based Complement Altern. Med. 12. https://doi.org/10.1155/2012/485042. Article ID 485042.
Lu, Q.Y., Summanen, P.H., Lee, R.P., Huang, J., Henning, S.M., Heber, D., Finegold, S.M., Li, Z., 2017. Prebiotic potential and chemical composition of seven culinary spice extracts. J. Food Sci. 82 (8), 1807–1813.
McGahon, A.J., Martin, S.J., Bissonnette, R.P., Mahboubi, A., Shi, Y., Mogil, R.J., Nishioka, W.K., Green, D.R., 1995. The end of the (cell) line: methods for the study of apoptosis in vitro. Methods Cell Biol. 46, 153–185.
Morris, G.M., Huey, R., Lindstrom, W., Sanner, M.F., Belew, R.K., Goodsell, D.S., Olson, A.J., 2009. AutoDock4 and AutoDockTools4. Automated docking with selective receptor flexibility. J. Comput. Chem. 30 (16), 2785–2791.
Mosmann, T., 1983. Rapid colorimetric assay for cellular growth and survival: application to proliferation and cytotoxicity assays. J. Immunol. Methods 65, 55–63.
Mota, N.S.R.S., Kviecinski, M.R., Zeferino, R.C., de Oliveira, D.A., Bretanha, L.C., Ferreira, S.R.S., Micke, G.A., Wilhelm Filho, D., Pedrosa, R.C., Ourique, F., 2018. *In vivo* antitumor activity of by-products of *Passiflora edulis* f. *flavicarpa* Deg. Rich in medium and long chain fatty acids evaluated through oxidative stress markers, cell cycle arrest and apoptosis induction. Food Chem. Toxicol. 118, 557–565.
O'Boyle, N.M., Banck, M., James, C.A., 2011. Open Babel: an open chemical toolbox. J. Cheminf. 3 (33), 14.
Sherman, P.W., Billing, J., 1999. Darwinian Gastronomy: why We Use Spices: spices taste good because they are good for us. Bioscience 49 (6), 453–463.
Siddiqui, S., Ahamad, M.S., Jafri, A., Afzal, M., Arshad, M., 2017. Piperine triggers apoptosis of human oral squamous carcinoma through cell cycle arrest and mitochondrial oxidative stress. Nutr. Canc. 69 (5), 791–799.
Trott, O., Olson, A.J., 2010. AutoDock Vina: improving the speed and accuracy of docking with a new scoring function, efficient optimization, and multithreading. J. Comput. Chem. 31, 455–461.
Zhang, J., Zhu, X., Li, H., Li, B., Sun, L., Xie, T., Zhu, T., Zhou, H., Ye, Z., 2015. Piperine inhibits proliferation of human osteosarcoma cells via G2/M phase arrest and metastasis by suppressing MMP-2/-9 expression. Int. Immunopharmacol. 24, 50–58.